CASE STUDY ON A LARGELY-DEFORMED GEOTEXTILE-REINFORCED SOIL RETAINING WALL INDUCED BY RECENT HEAVY RAINFALL IN JAPAN

J. Hur[1], and S. Shibuya[2]
[1]Graduate student, Department of Civil Engineering, Kobe University, Japan;
Email: hur@stu.kobe-u.ac.jp
[2]Professor, Department of Civil Engineering, Kobe University, Japan;
Email: sshibuya@kobe-u.ac.jp

ABSTRACT

In the field of geotechnical engineering, the mitigation of geo-hazards induced by heavy rainfall is a common issue in many Asian countries, where the human as well as industrial activities are concentrated over a densely-populated deltaic plane surrounded by mountains. Geo-hazards encountered in such Asiatic regions are highlighted by large-deformation or often catastrophic failure of natural slopes and the geo-structures located in a valley. In this paper, two case studies dealing with reinforced earth wall are described. It should be mentioned that heavy rainfall was the trigger for the trouble encountered. In these case studies, the causes of the excessive deformation, together with the results of numerical examination into countermeasures are described in detail. First, various site investigations and laboratory tests were carried out in order to manifest the current state of the reinforced soil retaining wall. Second, the deformation behavior of the wall was simulated by performing numerical analysis. Finally, an appropriate countermeasure to prevent further development of the wall deformation was proposed by predicting the stress-strain behavior of the reinforced soil retaining wall with the remedial work.

Keywords: Case study, geotextile, heavy rainfall, site investigation, numerical analysis

INTRODUCTION

Figure. 1 shows the rainfall record in Japan over the last three decades. No doubt that the country has been suffering from an abrupt intensification of rainfall attack over the last decade or so. In Japan at least, the mechanical interpretation for the occurrence of large-deformation or failure of natural slopes and geo-structures is poorly understood, since i) neither soil profile nor the soil properties at the troubled site is usually available, ii) in the design of embankments for road and housing, for example, some increase in strength of unsaturated soil due to suction is implicitly ignored, hence iii) the mechanical behavior of soils at unsaturated state is poorly understood owing to insufficiency of practical implications. Above all mentioned, a bad-will of practicing engineers who tend to conceal real facets involved in the problem is an obstacle against the sound development on engineering discipline for mitigating such geo-hazards.

It is crucially important for practicing engineers to gain invaluable experience from well-documented case history as such. The objective of this paper is hopefully to provoke a lively discussion on how to mitigate geo-hazards induced by heavy rainfall with particular reference to reinforced earth walls. In documenting these case studies, the deformation and strength characteristics of unsaturated soils are in depth examined in the laboratory by focusing the effects of soil suction on elastic stiffness at very small strains as well as the strength at large strains.

An engineering practice (or methodology) in common for manifesting the cause(s) of largely-deformed (or failed) natural slopes and reinforced earth walls is discussed. Lessons learnt from each of these case studies, including the countermeasures employed are exposed.

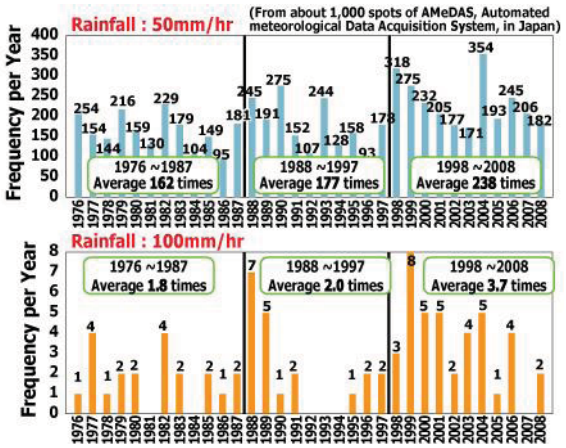

Fig. 1 Rainfall record in Japan over the last three decades

CASE HISTORIES

The outlines of these two case records are shown in Table 1. In each case study, the type of structure, the engineering problem cited, the site investigation performed and the analytical method employed are summarized. It should be mentioned that heavy rainfall was the trigger for the trouble encountered in the two cases.

Table 1 Outline of the case studies

Division	Case 1	Case 2
Type of Structure	Reinforced earth wall with geo-synthetics	Reinforced earth wall with geo-synthetics
Event	Compressive failure of concrete panels	Large deformation of wall facing
Trigger	deformation of weak soil layer on soaking	deformation of under compacted soil layer
Site Investigation	HR-SW, Direct shear box test, Soaking test	HR-SW, Direct shear box test, Soaking test
Analysis	Stress-deformation analysis (2D FEM)	Stress- deformation a nal.(2D&3D FEM)

CASE 1: LARGELY-DEFORMED REINFORCED EARTH WALL WITH GEOTEXTILE

Outline

Interpretation of the mechanical behavior of a severely damaged reinforced earth wall comprising geotextile with a concrete panel facing was carried out. The background and cause of the damage are discussed based on the results of site investigation. The engineering properties of the fill were examined by performing various in-situ and laboratory tests, including the high resolution surface wave survey (HR-SW survey), suspension P-S velocity logging test (PS-logging), radioactive logging(radio isotope logging, RI-logging), soaking test, the direct shear box test (DSB), bender element test (BE test), etc.

In Japan, reinforced earth wall with geotextile is popular for the construction of roads in mountain area. The use of reinforced earth comprising the vertical or very steep facing is advantageous in saving the construction cost compared to bridges, for example. In the case of reinforced earth wall comprising geotextile with the concrete panel facing, however, it involves a great difficulty in compacting properly the portion of the fill adjacent to the wall facing. As a result of loose compaction near the wall, the wall facing may be damaged by compressive force and/or could be completely destroyed due to the active failure of the fill (for example, refer to Tatsuoka.et al., 1997). Figure 2 shows typical damages for reinforced earth in general. In case of flexible reinforced earth without any concrete facing, a local failure involving excessive compressive deformation would take place at the bottom portion, which in turn may trigger the overall active slip failure in a progressive manner (refer to Tatsuoka et al., 2000). Conversely, when the reinforced earth with concrete panels comprises a poorly compacted (or soft soil) layer at the time of construction, a connection between the concrete panel and reinforcement material (i.e., the metal strip or geotextile) would be destroyed owing to the downward tension force at the connection, which eventually may bring about complete failure of the wall.

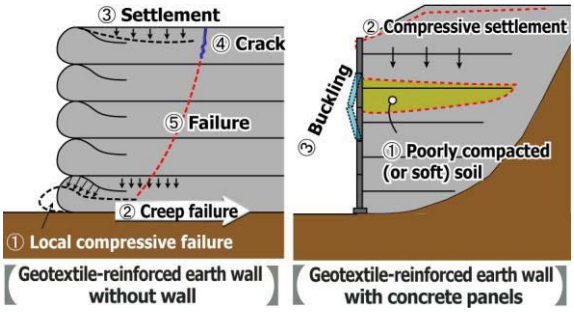

Fig. 2 Typical damages of reinforced earth walls

The severely-damaged reinforced earth wall 150 long with a maximum height of 15m is situated at the end of the main line of Tottori expressway. It is bounded by valleys in the mountain area in Hyogo Prefecture, Japan. The wall is a reinforced earth wall with geo-textile constructed using the local soils. The details of the geotextile-reinforced soil retaining wall are shown in Fig. 3.

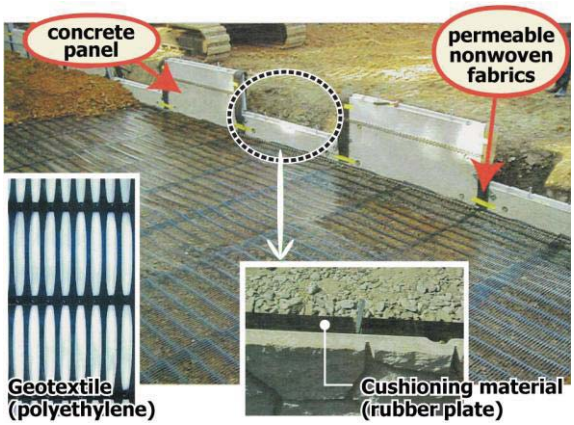

Fig. 3 Details of the geotextile-reinforced soil retaining wall (Case 1)

In November 2006, irregular deformation of the wall was observed at the middle stage of the construction. Accordingly, a partial reconstruction involving cement stabilization of the fill was carried

out after removing some parts of the reinforced earth wall, which is called "the first remedy" in this paper.

In April 2007, an unexpected deformation of the wall was again observed at the eleventh stage of the construction being close to the final construction stage. Therefore, after demolishing some parts of the wall, the wall was reconstructed with cement stabilization of the upper part of the fill.

Furthermore, a horizontal drainage layer was installed in the middle part of the wall. In this paper, this reconstruction of the wall is called "the second remedy".

On the other hand, the locations for the HR-SW survey, PS-logging, RI-logging, boring and the standard penetration test (SPT) are indicated in Fig. 4. The wall height at the severely damaged portion was approximately 15m. As described earlier, the parts of the fill for the first and second remedies had been improved by cement injection using a dry weight Portland cement of 50kg/m^3. The drainage layer was sandwiched between these two cement-mixed layers.

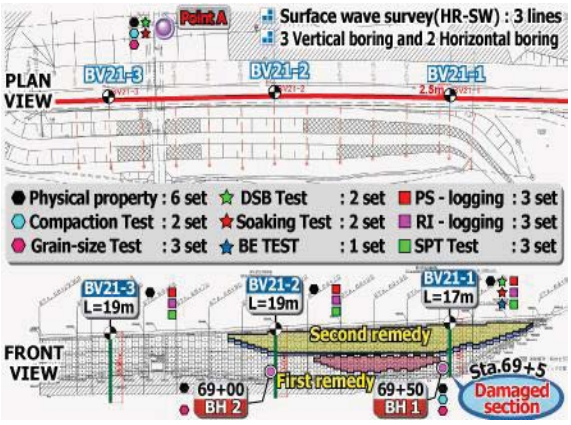

Fig. 4 Front and plan views of the site

Note that the severely damaged portion of the wall is surrounded by the improved soil with a low-permeability and the bedrock. In addition, there is a small valley behind it. The construction of the wall was finally completed in November, 2007. However, the field observation clearly indicated that the deformation of the wall showed no tendency to stabilize with time. A case study was hence commissioned in order to evidence the cause(s) of the wall damage, and also to examine effective countermeasures to re-stabilize the wall.

Figure 5 shows some pictures of the reinforced earth wall cited, including the severely damaged portion. The outwards deformation at the damaged portion on the wall was on-going by showing the horizontal displacement to reach the value as large as 217mm. The concrete panel wall had been constructed by using a high-density polyethylene geotextile. Based on the observation, a type of wall damage due to the existence of a poorly compacted soil layer was strongly suspected (refer to Fig. 2).

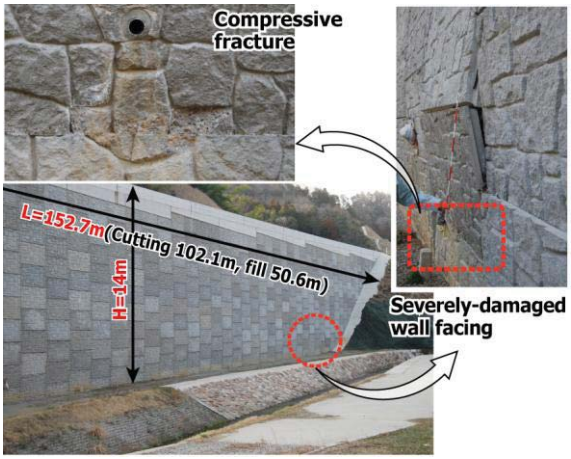

Fig. 5 Severely damaged portion

In-Situ and Laboratory Tests

The HR-SW survey was carried out to figure out the 2D profile of the elastic wave velocities, i.e., S-wave and P-wave velocities (V_s and V_p) of the fill, together with the foundation. Fig. 6 shows the profiles of V_s and V_p with depth for the 160m long survey line L1. In general, the V_s increase with depth, since in-situ overburden stresses increase with depth. However, a low-velocity layer was observed for V_s near the severely damaged section at BV21-1 (n.b., elevation: approximately 240m, distance: 110~115m). The decrease in V_s strongly suggests some reduction of the magnitude of stresses at the deformed section. On the other hand, the dashed curve in the profile of V_p represents the boundary associated with V_p = 1500m/s, noting that the specific condition of V_p = 1500m/s is applicable to saturated soil. Accordingly, it may be surmised that the state of soil behind the damaged panels is close to saturation.

A noticeable decrease in V_s near the deformed section was indicated by the HR-SW survey. Therefore, a down-hole PS-logging was carried out to directly measure the profile of V_s with depth. Similarly, RI-logging using the Gamma Ray attenuation technique was performed for profiling the variations of wet density, ρ_t, and the natural water content, w_n, with depth. Fig. 7 shows the profiles of V_s, N-value, ρ_t, ρ_d and w_n at three locations of BV21-1, BV21-2 and BV21-3, respectively (see Fig. 4). As seen in Fig. 7, the horizontal layer over the depths roughly from 10m to 13m for the length between BV21-1 and BV21-2 is seemingly soft by showing higher water content with the relatively low values of V_s, N-value, and ρ_d. The supposed soft soil layer corresponds to the portion characterized by the low-velocity from

surface wave survey. Meanwhile, both of V_s and N-value appear relatively larger for the soil layer improved by cement-mixing (i.e., the portions for the first and second remedies, see Fig. 4).

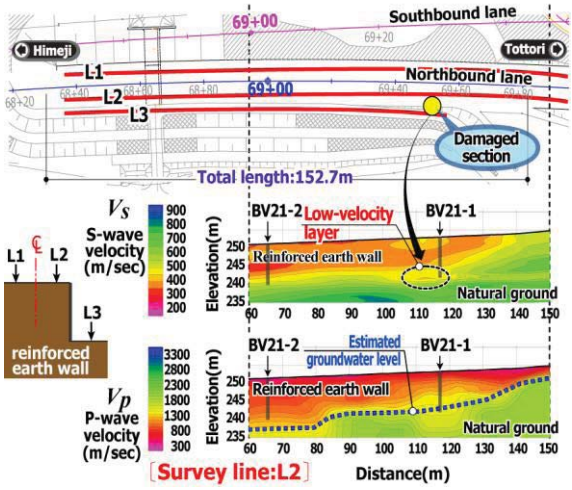

Fig. 6 Results of HR-SW survey

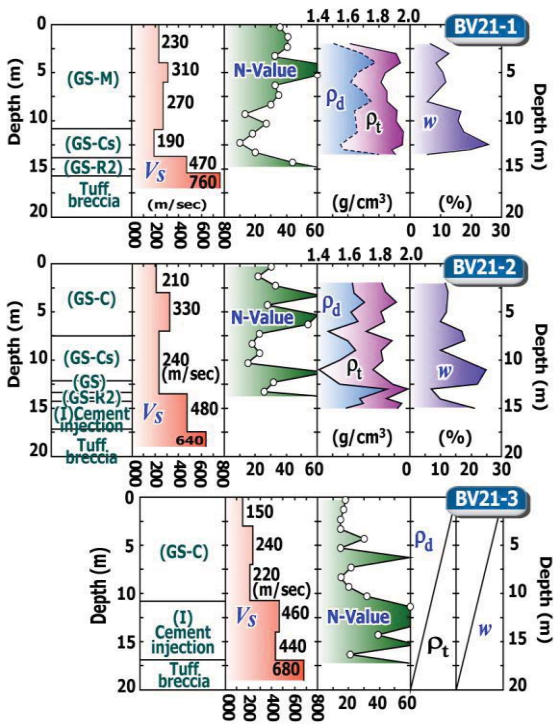

Fig. 7 Distribution of physical properties of the fill

The physical properties, together with the compaction characteristics of the fill material were measured using disturbed soil samples retrieved at three locations; i.e., the two samples at BH1, BH2 and the other sample at point A on the slope (see Fig. 4).The soil at BH1 corresponds to the severely damage portion. Similarly, the soil at BH2 represents the fill material on the same level as the soil at BH1. On the other hand, the soil at point A on the slope may be regarded as sourcing for the filling. Fig. 8 shows the grain size distribution of these three samples. It is obvious in this figure that the soils from BH1 and BH2 are much finer in grain size by showing the fines content, F_c = 49.0% and 40.2% for BH1 and BH2, respectively, whereas F_c = 25.2% at point A.

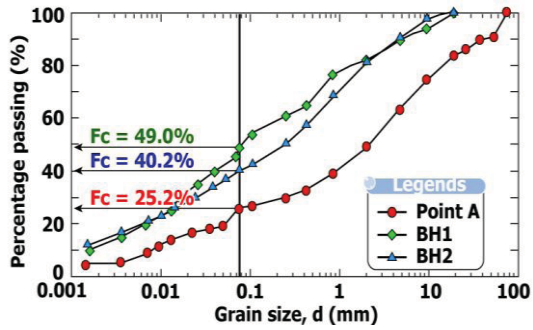

Fig. 8 Grain-size distribution

Figure. 9 shows the compaction curves of two samples at point A and BH2. The maximum dry density, $\rho_{d\ max}$, of the BH2 sample was far smaller than the other sample (n.b., $\rho_{d\ max}$=1.572 g/cm^3 for the BH2 sample and $\rho_{d\ max}$=1.832 g/cm^3 for the other), whereas the optimum water content was higher (n.b., w_{opt}=23.6 % for the BH2 sample and w_{opt}=15.6 % for the other. It should be mentioned that the entire fill was constructed by using the same method. In addition, the controlled value for the density was set to 0.9$\rho_{d\ max}$ based on the compaction curve similar to that of the sample at point A. It is now almost certain that the soft soil layer with larger amount of fines, and having lower values of V_s, N-value and ρ_d is responsible for the damage of the wall as shown in Fig. 2.

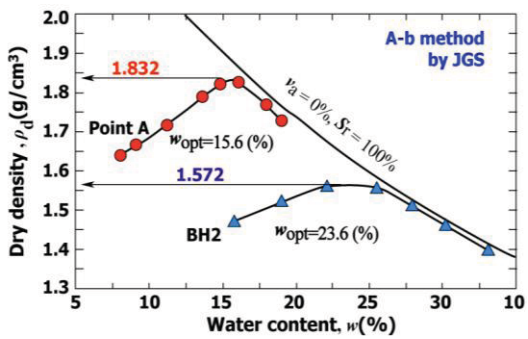

Fig. 9 Compaction curves

As shown in Fig. 10, the $V_{s,lab}$ from the BE test almost coincided with $V_{s,f}$ at the relevant depth when the sustained σ_v of the laboratory sample was 22.5kPa, noting that the σ_v of 22.5kPa accounts for approximately one-tenth of in-situ overburden pressure at prescribed depth. In an attempt to obtain

the shear strength at the damaged section, the constant-pressure DST (for the details of apparatus, see Shibuya et al., 2005) was performed.

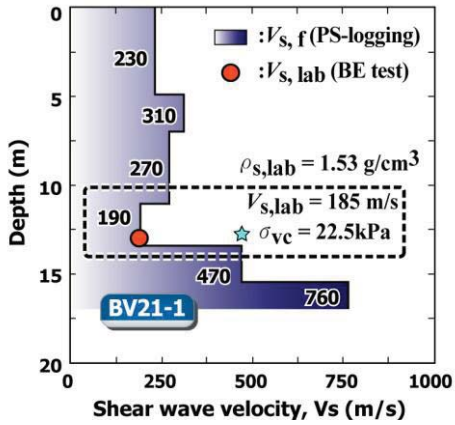

Fig. 10 Comparison of V_s between PS-logging and BE test in the laboratory (Jung et al, 2010)

The relationship between the shear stress and the horizontal displacement is shown in Fig. 11, in which similar result of the sample from point A is also shown for comparison. The maximum shear stress, τ_{max}, of 17kPa was very small for the sample at the damaged section, bearing the overburden height of the embankment of about 10m in mind.

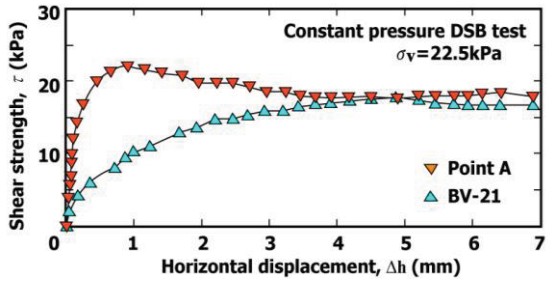

Fig. 11 τ-Δh relationships in constant pressure DST

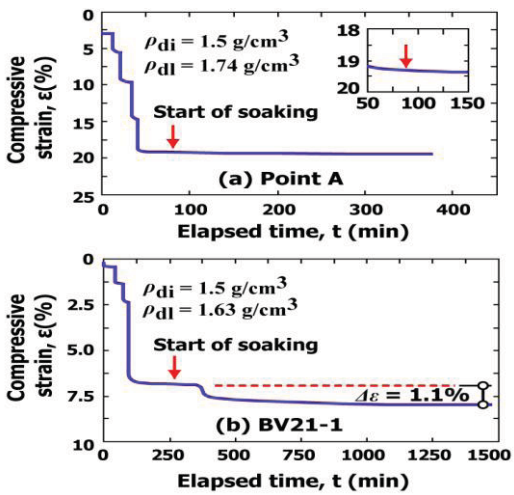

Fig. 12 Results of soaking test at v =200kPa

The stress-displacement curve exhibited no peak for the sample, whereas it showed a higher strength for the other sample comprising less fines.

According to the results of site investigations performed, the soil at the damaged section is currently saturated (see Fig. 6). This means that the initially unsaturated soil at compaction is soaked gradually possibly due to seepage flow into the fill. Soaking test was, therefore, carried out in an attempt to examine the deformation behavior during the process of soaking. The results of soaking test are shown in Fig. 12. On soaking, the sample at the deformed section exhibited a considerable amount of settlement with time to reach the compressive strain of 1.1 % over a period of one day. Conversely, no volume change was observed for the other sample.

Scenario of Wall Damage

The results of in-situ and laboratory tests have revealed the fact that a 3m-thick weak soil layer extends behind the damaged section of the wall. The in-situ state for the weak soil layer may be characterized with unexpectedly low values of V_s, ρ_d and the SPT N-value. In addition, the soil properties can be characterized by the occurrence of a considerable amount of settlement on soaking. Fig. 13 shows the picture inside the wall at the deformed section. A space was found underneath the geotextile, suggesting that the weight of the fill above the geotextile was partially supported by the tension force of geotextile. In this paper, the new wording of "hammock state" is conveniently used for describing it.

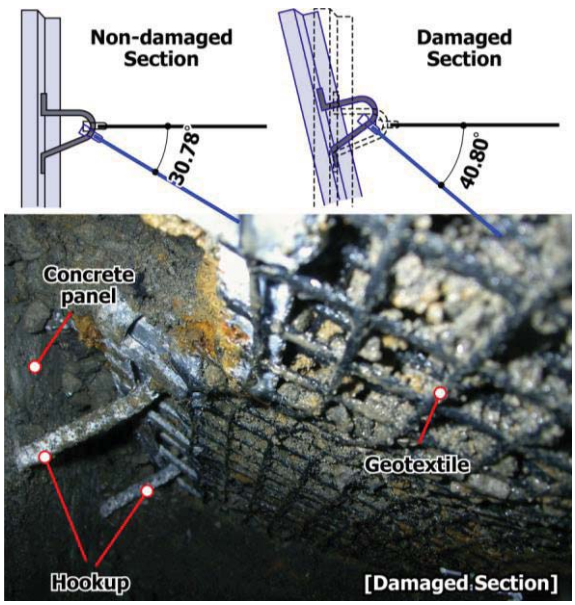

Fig. 13 Pictures inside reinforced earth wall

Based on this observation, the background as well as the mechanical interpretation for the damage of the wall can be postulated as an image shown in Fig. 14. It may be described such that:

i) a considerable amount of subsidence took place over the 3m-thick weak soil layer in the lower part of the reinforced earth due to seepage of rainfall water,

ii) the weight of the upper fill was partially supported by the geo-textile hooked on the concrete panels, and

iii) the concrete panels associated with the hammock state were severely damaged by the unexpectedly large downwards compression force triggered by the tension force of the geotextile.

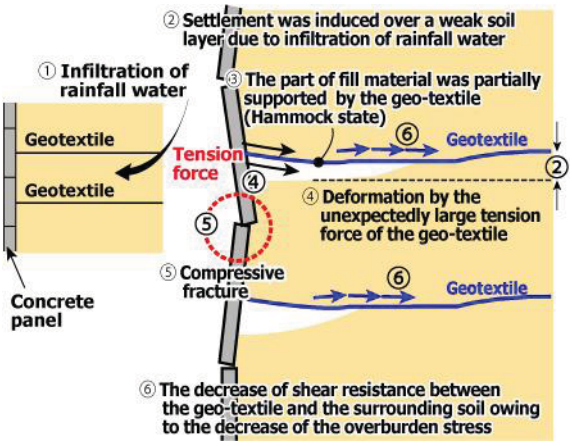

Fig. 14 Mechanical behavior of a largely-deformed reinforced earth wall with geo-textile

Once the hammock state was reached inside the wall, the overburden stress corresponding to the hammock state in the fill will be dramatically reduced, which in turn would bring about some decrease of the shear resistance between the geo-textile and the surrounding soil. The notion is strongly supported by the results of laboratory tests that the estimated σ_v at the deformed section was as small as one-tenth of the supposed σ_v (see Fig. 10).

Numerical Simulation

Prior to considering countermeasures to re-stabilize the wall, a numerical analysis was carried out in order to simulate the development of the large deformation that took place on the reinforced earth wall. As stated earlier, the wall was re-constructed twice. However, the wall deformation showed no sign to cease even at the final stage of the construction. As seen in Fig. 15, the range for the maximum value of horizontal deformation was 150 to 200mm. This corresponds to deformation rates of 1.0 to 1.5% against the height of the wall.

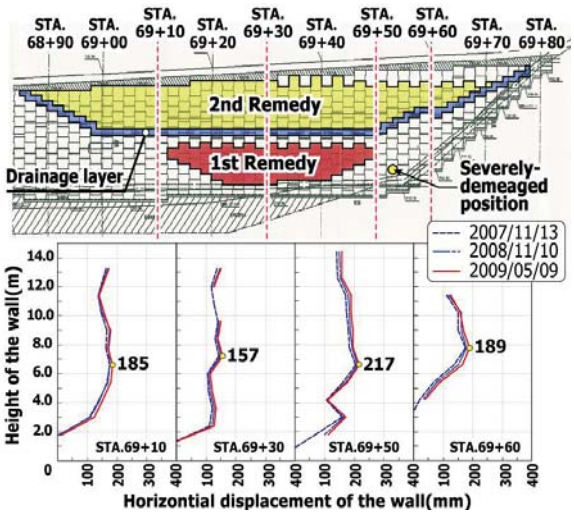

Fig. 15 Observed deformations of the wall facing

Figure 16 shows a representative cross section used for the numerical analysis. Note that the cross section of STA69+50(see Fig. 15) corresponds to the portion where the wall was severely damaged. As shown in Fig. 17, the geotextiles were modeled using "GEOGRID ELEMENT" of the PLAXIS.

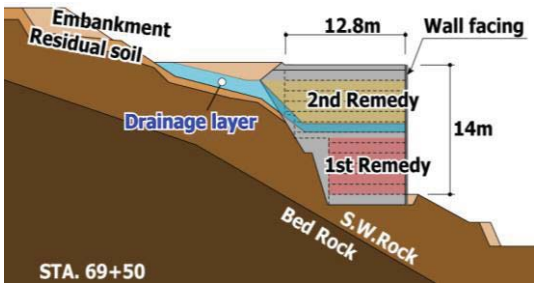

Fig. 16 Cross section used in the numerical analysis

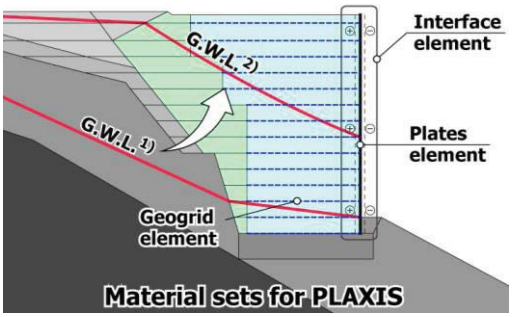

Fig. 17 Element types employed for the analysis by PLAXIS

Figure 18 shows how the reinforced earth wall was deformed according to the increase in the ground water level. The maximum amount of displacement with and without rain is 211.5mm and 148.3mm, respectively. This observation demonstrates that the infiltration water permeating the reinforced earth wall has a strong influence on the movement of the wall.

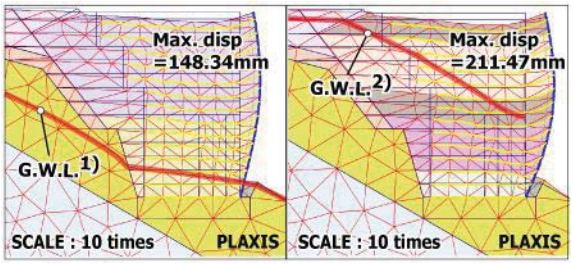

Fig. 18 Deformed meshes due to the increase in a water level

Figure 19 shows the results of an analysis performed for two cases, i.e., the case of normal geotextile and the other case of geotextile in the condition of Hammock. Based on the observation, the hammock condition was assumed over the lower part of the wall comprising the soft soil layer. The effect of Hammock was significant in that large deformation was observed near the wall by showing the maximum shear strain increment almost ten times that of the normal condition.

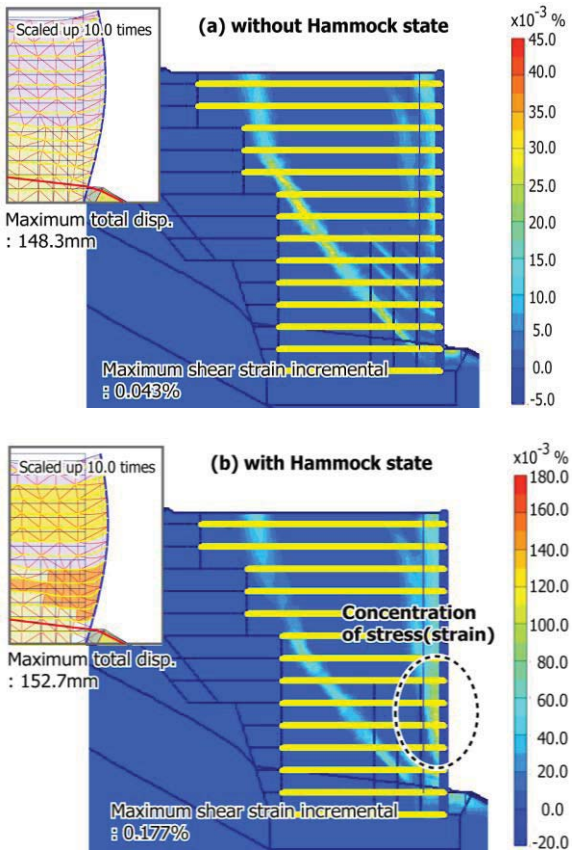

Fig. 19 Incremental shear strains in the fill, together with the deformed meshes near the wall facing

As well depicted in Fig. 20, the large deformation of the wall may be induced with the sequence of events in the following. First, the filling materials with a high compressibility existed on some layers inside the backfill. Second, rainwater and the water in a valley infiltrated into the layers, which in turn induced compression settlement. As a result of the generation of settlement in the weak soil layer, so-called 'Hammock state', in which the weight of the upper filling was partially supported by the geotextiles, was gradually formed. This condition generated high tensile force to the geotextiles, which in turn induced stress concentration on the concrete panel connected to the high-tensioned geotextiles. As a consequence, a type of compression failure took place on the concrete panels.

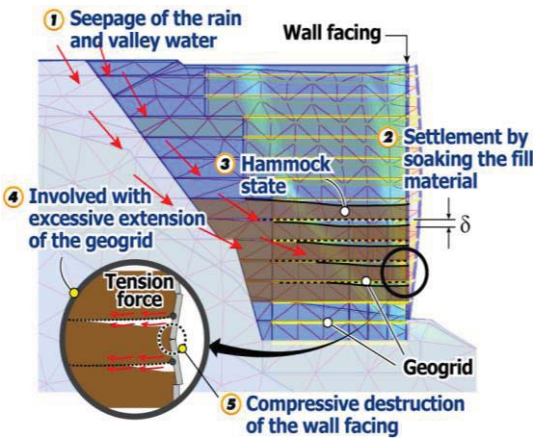

Fig. 20 Sequence for the development of wall damage

Countermeasures

Figure 21 shows the overall scheme of counter-measures employed. Based on the results of site investigation, together with numerical simulation, it was needed to prevent any seepage water from infiltrating into the embankment so that a geosynthetic drain was first installed as an urgent, and hopefully permanent, remedial work (see Fig. 21).

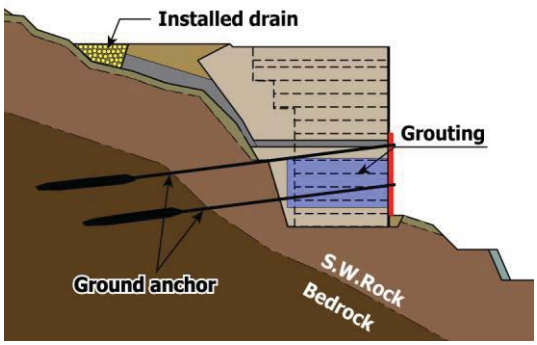

Fig. 21 Scheme of countermeasures employed for re-stabilizing the wall

Figure 22 shows the implementation of the geo-synthetic drain with gravels. As seen in Fig. 23, the drain system was highly effective in respect that a considerable amount of seepage water from a small valley behind was discharged over a substantially long period after each rainfall. Second, cement-grouting was implemented for preventing further development of compression of the soft soil layer, hence to avoid further damage to the wall facing. Eventually, ground anchors were planted in order to enhance the overall stability of the wall. The minimum rate for the safety factor, F_s, was 1.51 after implementing the ground anchors, the value of which exceeded F_s =1.25 of the allowable rate for the safety factor in design. Fig. 24 shows the picture after the remedial work. In April 2010, the wall was successfully open to the public service.

Fig. 22 Installing geosynthetics drain system

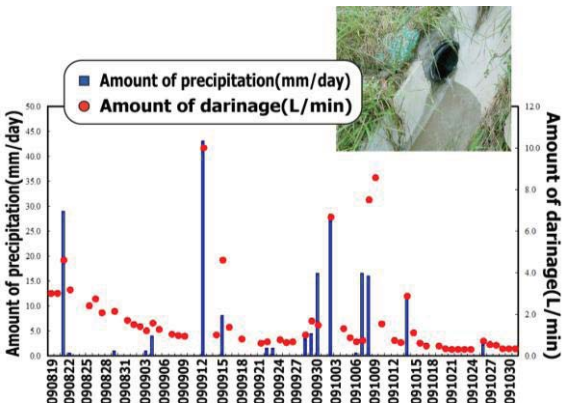

Fig. 23 Discharge by geosynthetics drain system

Lessons Learnt

In this case study, the wall damage was seemingly induced with successive development of compressive strain of 3m-thick weak soil layer at the lower part of the fill. The soil comprised larger amount of fines, and hence it was poorly compact. A scenario for the wall damage may be described such that a considerable amount of subsidence took place over the weak soil layer due to seepage of rainfall water, the weight of the upper fill was partially supported by the geo-textile hooked on the concrete panels, and the concrete panels associated with this "hammock state" were severely damaged by the unexpectedly large downwards compression force triggered by the tension force of the geotextile.

Bearing this scenario in mind, the following may be pointed out:

i) When the wall is constructed using local soils, care should be taken for the variation of the soil properties such as the grain-size distribution, the characteristics of compaction, stiffness, strength etc. These properties should frequently be examined in the laboratory, and the results should be properly considered for the scheme for the wall construction. Geotechnical engineers should be faithful to make a decision for discarding unsuitable soil for the filling.

ii) In the reinforced earth with concrete facing, the state of under-compaction is likely to take place for the portion adjacent to the wall. Extra care should be taken to achieve a thorough management of compaction work adjacent to the wall, in particular. Otherwise, a better geomaterial such as gravels may preferably be used.

iii) A performance-based design should be implemented urgently in the design manual for reinforced earth wall. If the deformation analysis considering the seepage water were performed prior to the construction, the trouble encountered in this case study could have been avoided.

iv) The countermeasures employed in this case study, i.e., the geosynthetic drain system to prevent any seepage water from infiltrating into the embankment, cement-grouting for reducing further development of compression of the soft soil layer and the ground anchors to enhance the overall stability of the wall, all worked well. The effects of the countermeasures to control displacements of the wall and the extensional strain of the geo-textile were successfully confirmed by 2D and 3D numerical analysis.

v) The importance of co-operation between wall engineers and geotechnical engineers was again cited in this case study.

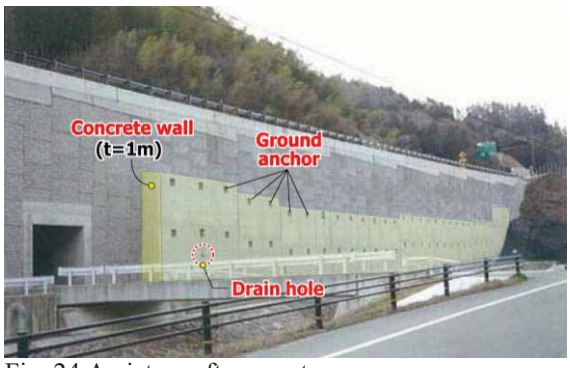

Fig. 24 A picture after countermeasures

CASE 2: LARGELY-DEFORMED GEOTEXTILE-REINFORCED SOIL RETAINING WALL

Outline

In general, when a reinforced soil retaining wall is built in a mountain valley showing catchment topography, seepage water from the rear as well as the surface of the filling is an intimidating factor for the stability of the wall. The site is shown in Fig. 25, in which the reinforced soil retaining wall was under construction in order to improve the linearity of the local road.

Comprehensive drainage facilities had already been implemented at the bottom of the valley. However, large deformation was observed in some parts of the wall in the course of the staged construction. The reinforced soil retaining wall is about 20m high. The construction of an embankment about 25m high in use for the roadbed was planned above the reinforced soil retaining wall (see Fig. 25). In June 2010, a horizontal displacement larger than 0.16m was observed on the reinforced soil retaining wall at the 32th stage of the construction of the wall. Preliminary numerical analysis suggested that when the embankment would be constructed without any remedies, the accumulated displacement of the wall would be double or triple as compared to present situation. Therefore, further construction was halted. In this case study, the current state of the reinforced soil retaining wall was examined by means of HR-SW survey, boring and a series of laboratory tests.

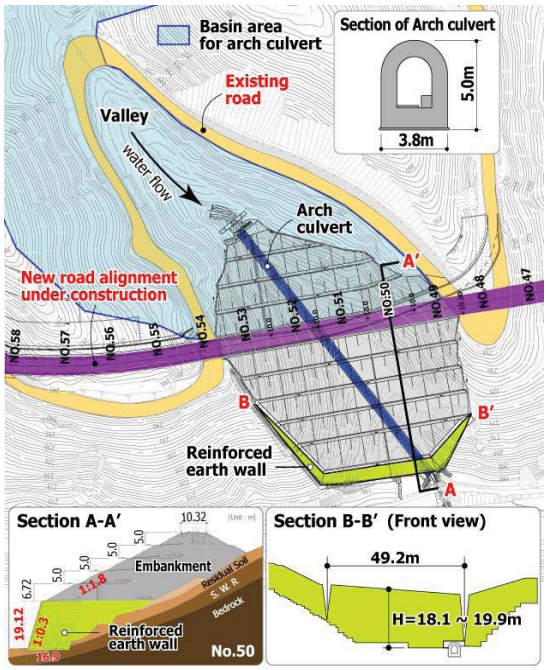

Fig. 25 On-site topography and reinforced soil retaining wall

In an attempt to evidence the cause of wall deformation, the deformation behavior of the wall involved with further construction of the embankment was predicted by means of numerical analysis, in which the sequence of construction, together with 3D topographical characteristics was properly considered. Efficient countermeasures not only stabilizing the reinforced soil retaining wall but also preventing any harmful deformation of the wall were also numerically examined.

The cited reinforced soil retaining wall with geotextile is about 20m tall and about 120m wide (refer to Fig. 25). Field instrumentations to observe the behavior of the reinforced soil retaining wall are a subsurface extensometer, a borehole inclinometer, a convergence meter of wall surface, strain gauges attached on geotextile, and a water level meter. As seen in Fig. 26, partial fractures of the metal facing were observed at the lower part above the concrete culvert due possibly to uneven settlement on and beside the concrete culvert. On the other hand, Fig. 27 shows the picture during an assembly work of reinforced soil retaining wall.

And then, Fig. 28 shows the variation of the horizontal and vertical displacements with time at several points over the facing. Large displacements were observed at No.50, for which the horizontal displacement exceeded 16cm and the settlement reached to 24.4cm over the middle part of the wall (T-5 and T-16). As indicated in Fig. 29, the extensional strain of the geotextile was observed at three levels, HF-1, HF-2 and HF-3.

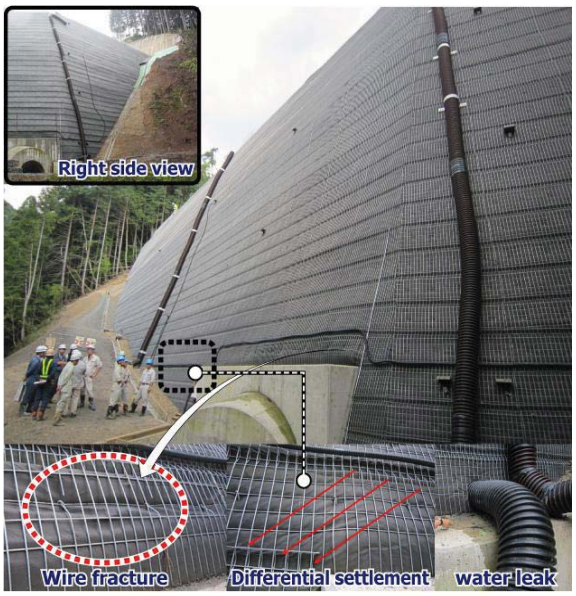

Fig. 26 Deformed reinforced soil retaining wall

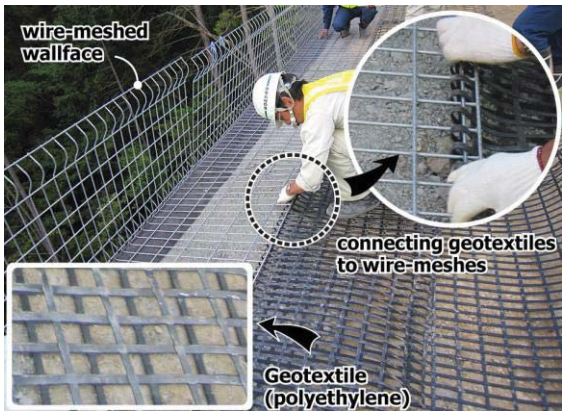

Fig. 27 A view of assembly work (Case 2)

Note that the strain in each geotextile was large at the portion close to the wall facing. This tendency may be attributed to the combined effects by the tensile force associated with the horizontal displacement of the wall and by uneven vertical displacement near the wall facing with metal frame. The strain increased from bottom to the top by showing the maximum strain of 0.7%, 1.2% and 1.4% at HF1, HF2 and HF3, respectively. It should be mentioned that the strain of 1.4% at HF3 accounts for 70% of the strain level corresponding to the upper limit of the safe domain (i.e., 1.987%).

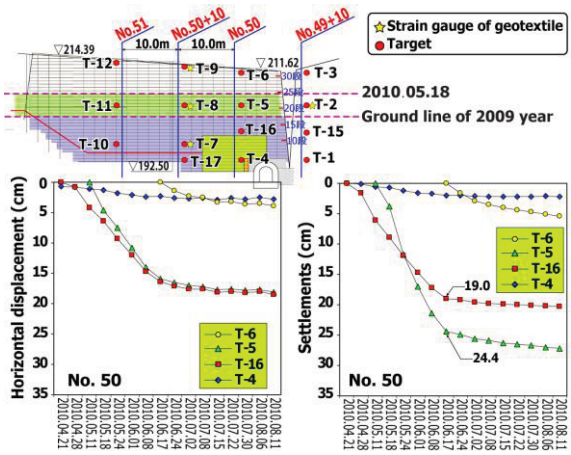

Fig. 28 Observed deformations of the wall

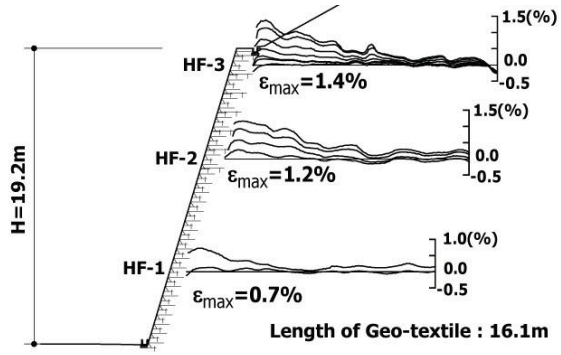

Fig. 29 Measured extensional strain of geotextile

In-Situ and Laboratory Tests

As can be seen in Fig. 30(a), a HR-SW survey along five survey lines was performed. Fig. 30(b) shows the 2D profile of S-wave velocity obtained from the survey. As a result of the survey, the existence of relatively low-velocity layer showing about 200m/s of S-wave velocity was found at the level around an altitude of 205m of the survey lines L1 and L2. In addition, the borehole sounding was carried out at two locations of K-6 and K-7. As a result, a loose layer was found at the middle of the filling (GL.-8~-11m).

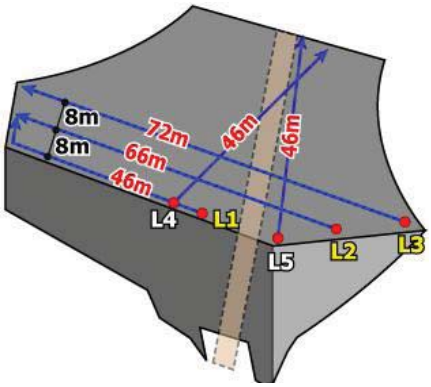

(a) Survey lines for HR-SW survey

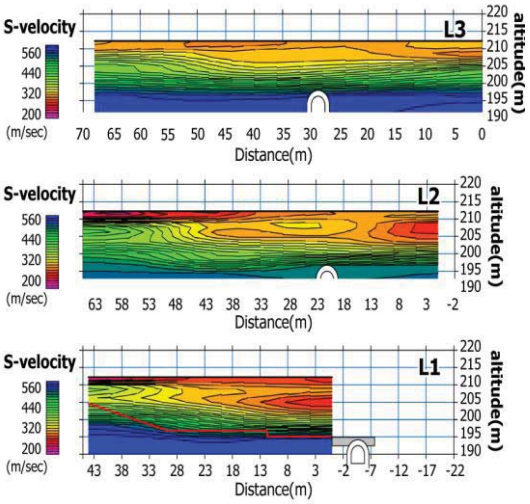

(b) Results of HR-SW survey

Fig. 30 In-situ HR-SW survey

Figure 31 shows the results of both the SPT N-value and the PS-logging. Note that the SPT N-value was relatively low (N=3~11) over the upper part from GL.-0 to GL.-9m. In the meantime, N-value from GL.-9m to the bottom was about N=7~21. Despite that the N-value at the lower part of the wall was relatively high compared to that at the upper part, a tendency for N-value to increase with depth was not observed. The degree of saturation from the upper part of the filling from GL.-0 to GL.-9m ranged from 57.8% to 76.3%. Meanwhile, the degree of saturation at the lower part of the filling was higher from 77.4% to the full saturation. A noticeable change in terms of the degree of saturation was found at an altitude of 205m.

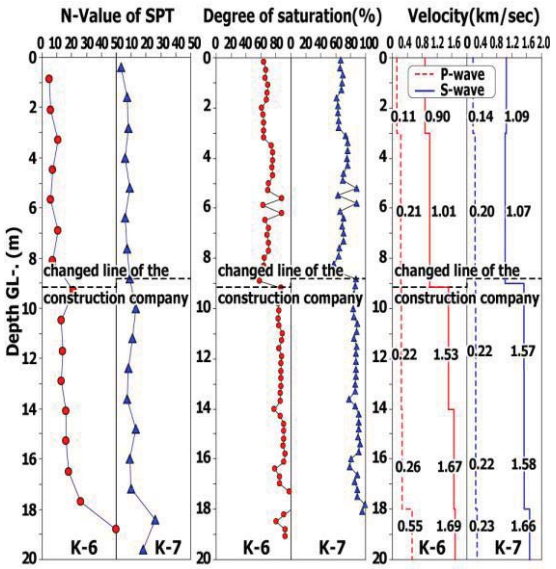

Fig. 31 Variations of N-value, degree of saturation and PS-velocities with depth

It should be mentioned that at this level, the construction company in charge was changed.

As indicated in Fig. 32, the reinforced soil retaining wall was constructed using the local soils that could be classified into four different origins.
The density control for the compaction work during construction was set to be over 90% of the maximum dry density from the compaction test in the laboratory.

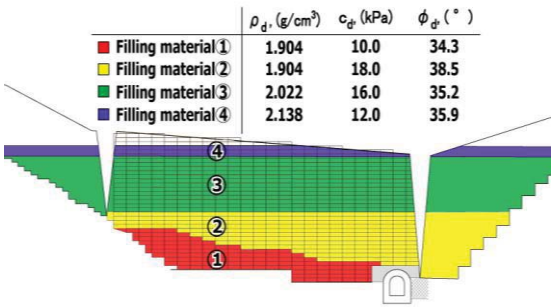

Fig. 32 Four types of geomaterials used for construction

Figures 33 and 34 show the results of grain size distribution curves and the compaction curves from different origins. The particle size distribution curves exhibited a considerable scatter. The filling material ①, the filling material ②, and core samples (K-6 and K-7) contain a relatively large amount of fine-grained particles. Meanwhile, the maximum dry density of the filling material ① and the filling material ② is 1,904kg/m^3, whereas the filling materials ③ and ④ exhibit the maximum dry density of 2,022 and 2,138kg/m^3, respectively. Compared to filling materials ③ and ④, the filling materials ① and ② exhibit lower dry densities and higher water contents. In addition, the compaction curve of filling material ② exceeded zero air void curve on wet side, indicating serious errors for the interpretation of the test result. It should be mentioned that the on-site compaction work was carried out by assuming a single compaction curve from the filling material ① with the maximum dry density of 1,904kg/m^3.

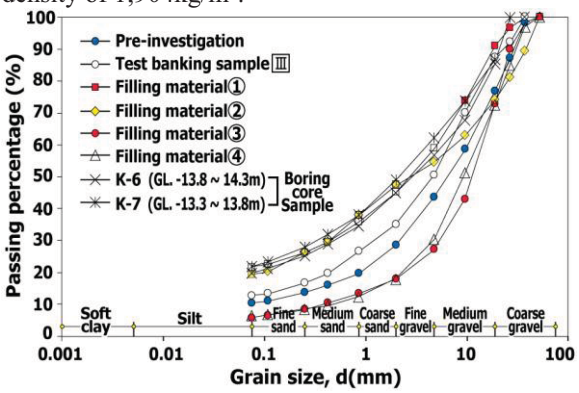

Fig. 33 Comparison of grain size distribution curves

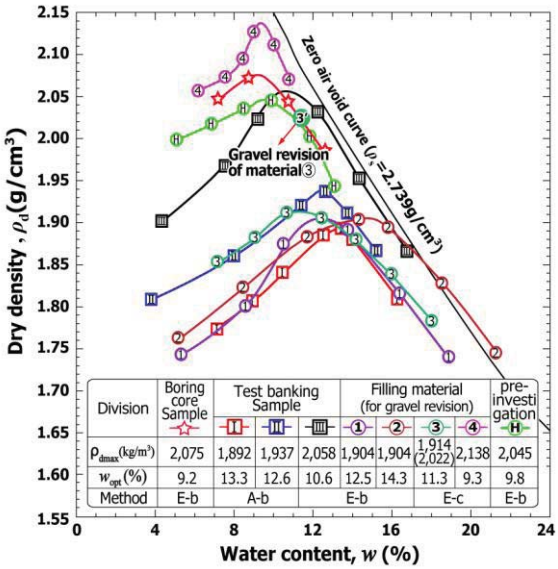

Fig. 34 Compaction curves

Figure 35 shows the results of revised in-situ degree of compaction, D_c. When the value of 2.075g/cm^3 of the maximum dry density of soils from boring cores (i.e., K-6 and K-7) was applied, the in-situ degree of compaction was 87% being lower than the prescribed lower limit of D_c=90% . Accordingly, a soaking test was carried out to examine the deformation behavior on wetting.

Figure 36 shows the result of the soaking test using two specimens from the boring While the sample with D_c=90% had no prompt volume changes, the other sample with D_c=87% showed a considerable amount of immediate settlement at 125 minutes after the soaking. A sort of collapse behavior may have been observed for the sample with D_c=87% due to the loss of matric suction. These results imply that the sample soil ① and ② used for the density control of the field compaction work was by no means a representative soil for the whole fill by showing a lower value in terms of the maximum dry density. Moreover, the soil when compacted loose with D_c=87% showed a collapse on soaking.

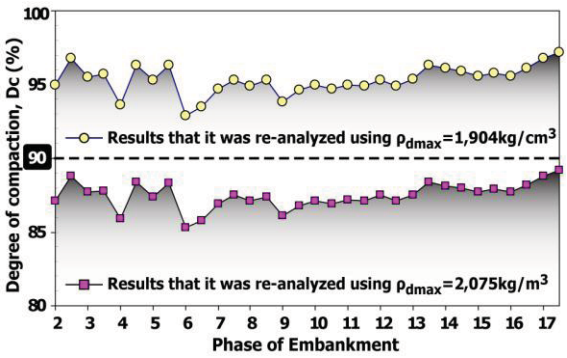

Fig. 35 Revised in-situ degree of compaction, D_c

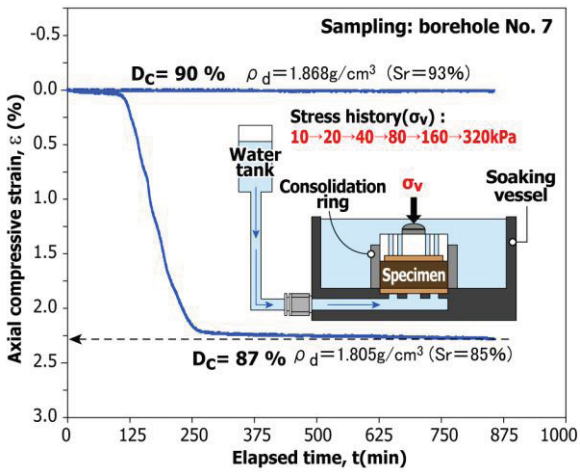

Fig. 36 Results of soaking test at σ_v=320kPa

Therefore, it may be surmised that a considerable amount of settlement occurred over the loosely compacted soil layer at the lower part in the event of rainfall and/or the attack of seepage flow from the rear side of the fill. Figure 37 shows the results of DST using boring core sample K-6. In the DST, two samples with the dry density of 1.6g/cm^3 and 1.8g/cm^3 were prepared. Note that the internal friction angle (ϕ_{ds}) was as high as about 36 degrees regardless of the density. In the meantime, the sample with the dry density of 1.8g/cm^3 showed a higher value of cohesion. It may be surmised that the degree of compaction of the cited soil does not influence much the strength, but the deformation on soaking was significantly affected by showing a type of collapse behavior for the loosely compacted sample.

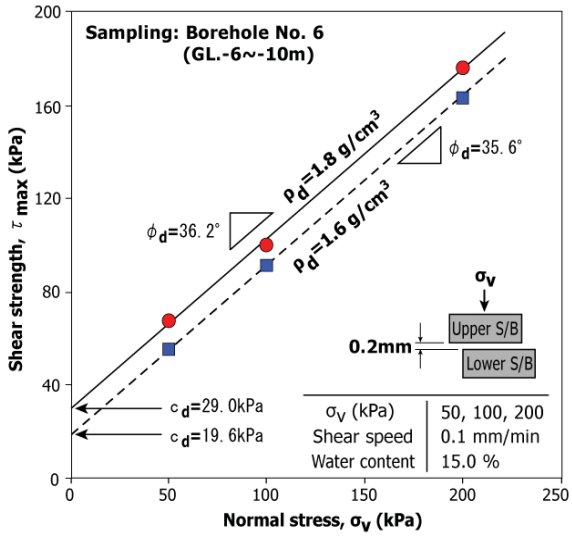

Fig. 37 Results of direct shear box test (DST)

Scenario of Wall Damage

As results of site investigations, it was estimated that the large deformation of the reinforced soil retaining wall was caused by compressive settlement of lower part of the fill in particular. The settlement was probably triggered due to seepage water infiltrated into the insufficiently compacted soil layer. Why the reinforced soil retaining wall exhibited large deformation may be described in the following:

i) the weak layer with a low degree of compaction remained inside the backfill,
ii) seepage water infiltrated into the soil layer, resulting in a considerable amount of settlement due to "collapse" of the loosely compacted soil layer and also due to the subsequent overburden stress during filling, and
iii) the settlement caused large deformation on the wall surface.

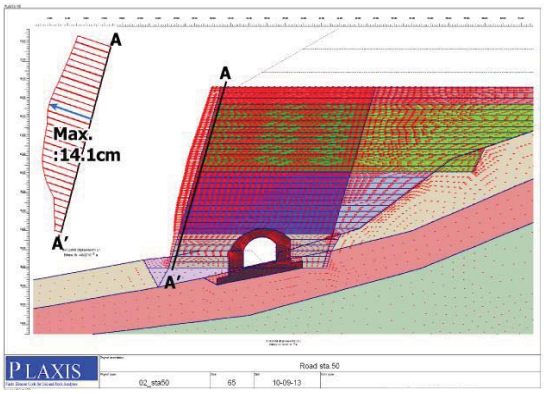

Fig. 38 Results of back analysis by using MC model

Numerical Simulation

As stated earlier, the development of further deformation of the reinforced soil retaining wall was expected when the construction of the roadbed embankment above the existing wall is constructed. In an attempt to examine the necessity of countermeasures against further deformation of the wall, the soil properties of the construction field were estimated by performing a back analysis. Fig. 38 shows a set of deformed mesh of the reinforced soil retaining wall generated for the back analysis with the PLAXIS. In the analysis, an elastic modulus of the filling material of 10MPa was first assumed. Second, two-dimensional or three-dimensional analysis was carried out using the soil properties estimated by the back analysis.

Figure 39 shows a tendency for the horizontal displacement of the wall surface expected when a road-bed embankment was put on the upper part of the wall. The maximum horizontal displacement was 42.1cm at the middle part of the wall surface.

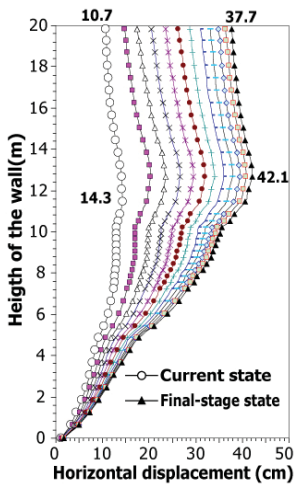

Fig. 39 Estimated horizontal displacement of the wall facing (No.50, 2D analysis)

As seen in Figs. 40 and 41, the results of three-dimensional analysis provided a smaller value as compared to the comparative result of two-dimensional analysis, since the three-dimensional analysis compiled the effects of the boundary conditions such as arching effects. Nevertheless, it was expected that the accumulated displacement of the wall surface will be double or even triple against the current state (see Fig. 40).

Figure 42 shows incremental shear strains associated with the construction of a roadbed embankment. This figure indicates that while the shear strain concentrates on the surface of the wall at an early stage of the roadbed embankment, it develops further inside of the filling at the final stage of construction. As described above, since the reopening of construction under the current situation will definitely induce serious instability of the whole structure, and also substantial increase of the wall deformation, a consensus was reached to apply countermeasures to re-stabilize the whole embankment prior to the reopening of the construction.

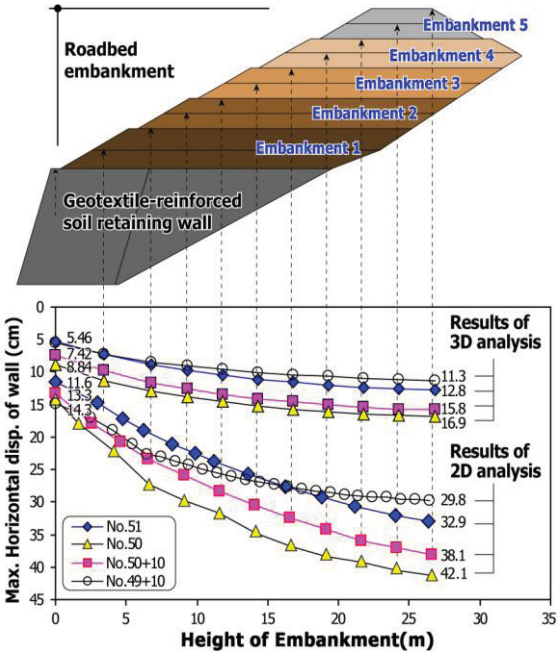

Fig. 40 Estimated horizontal displacements of the wall facing by 2D and 3D numerical analysis

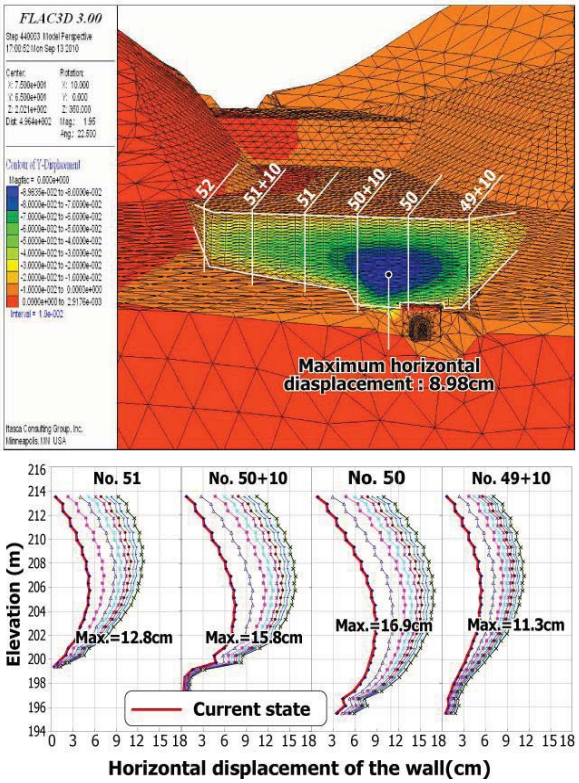

Fig. 41 Results of 3D analysis (FALC 3D)

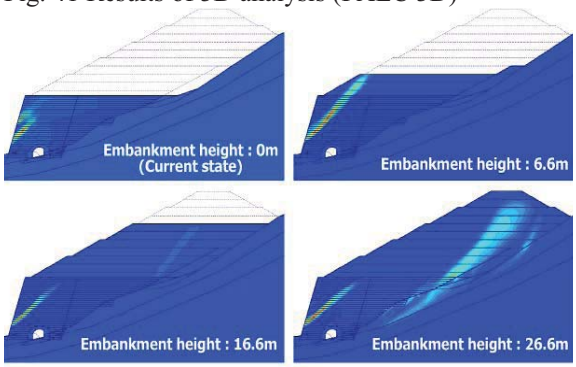

Fig. 42 Incremental shear strain in the fill (No.50, PLAXIS)

Countermeasures

The implementation of ground anchors was finally found most appropriate. The effects of the countermeasure using ground anchors are evaluated by means of numerical analysis. Figure 43 shows the reinforced section that was finally designed. In the design for implementing the counter-measure, the factor of safety for the overall embankment was assumed to be Fs=1.0. When installing ground anchors, the amount of initial pre-stress of anchoring, together with the size of the concrete wall at the front side of the reinforced wall were both considered in order to satisfy an allowable safety factor, F_{sa}, of 1.2 at ordinary times and of 1.0 in the event of earthquake.

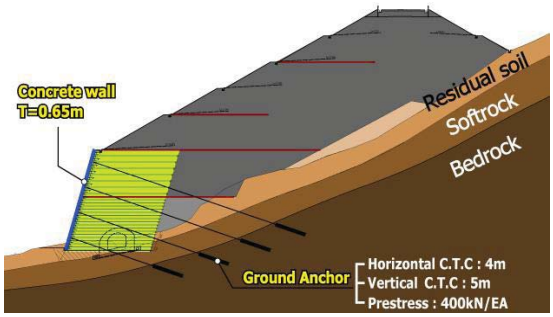

Fig. 43 Finally designed countermeasures

Figure 44 shows a comparison of the wall deformation for two cases with and without the application of the countermeasure. The compressive deformation of the wall surface from 14.3cm to 11.96cm was predicted on pre-stressing the anchors. This may be attributed to the materials' properties assumed in the analysis, for which the geomaterial in the fill was assumed as elasto-plastic material, together with the geotextile, anchors, and the reinforced wall being postulated as elastic material. At an early stage of the construction, the maximum horizontal displacement was observed at 12m to 13m high of the wall. However, towards the final stage of the construction, it was observed at the crown edge. The maximum of the horizontal displacement with ground anchors was reduced to 23.4cm at crown edge, which was almost half of 42.1cm for the case without the countermeasure.

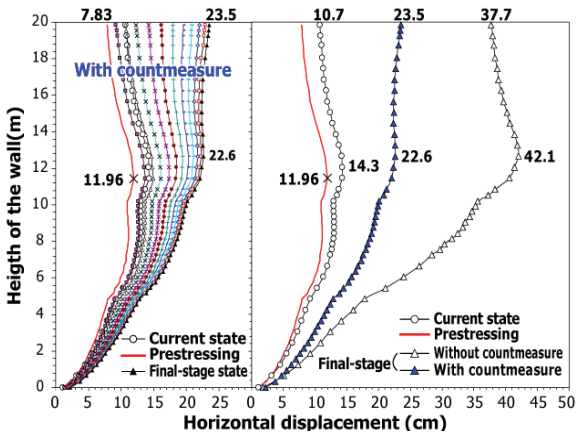

Fig. 44 Behavior of wall facing with and without countermeasure

Figure 45 shows the development of strain of the geotextile with and without the countermeasure. In the case of shiftlessness, the extensional strain of the geotextile reached to about 3%. Conversely, the effect of ground anchors was significant by showing the strain reduced down to about 1.5%. Fig. 46

shows the generation of shear strain. It can be observed that after applying the countermeasure, the increment of shear strain inside the fill is negligible. The implementation of ground anchors with concrete wall is expected to reduce much the danger for the active failure.

Figure 47 shows the picture after the counter-measures work.

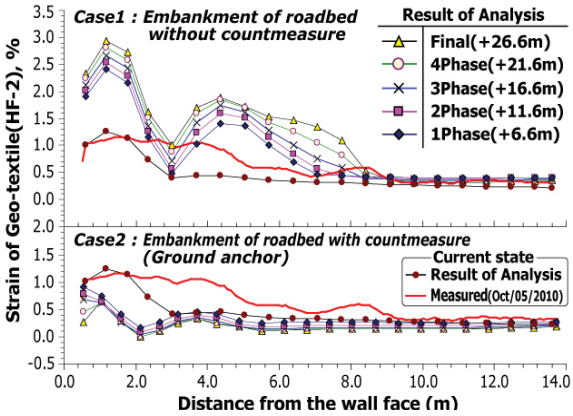

Fig. 45 Development of extensional strain of geotextile

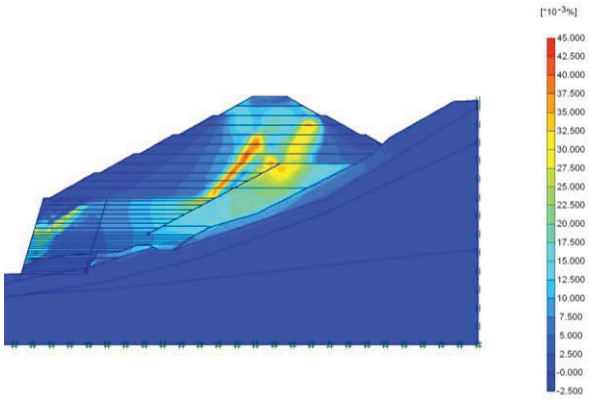

(a) Without countermeasure

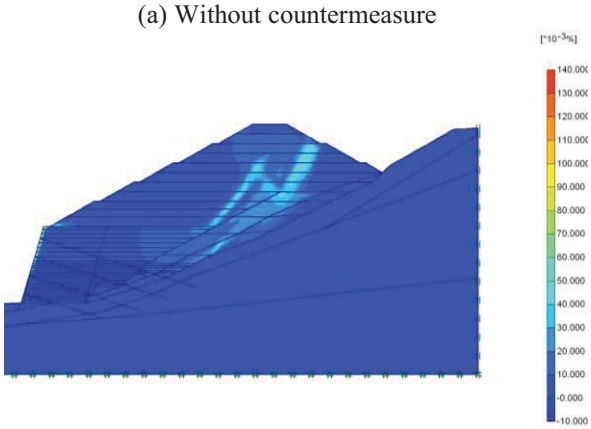

(b) With countermeasure

Fig. 46 Incremental shear strain rate at No. 50+10

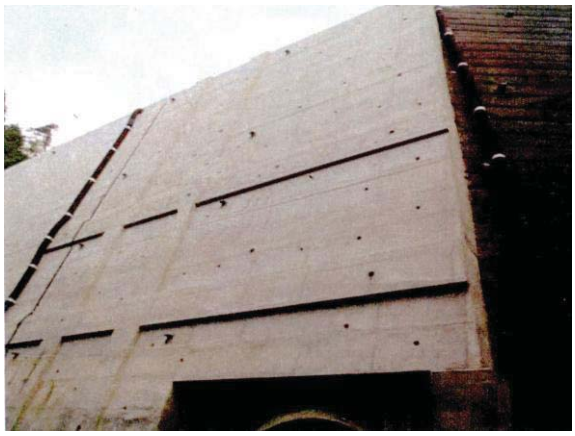

Fig. 47 A picture after countermeasures

Lessons Learnt

The scenario for the large-deformation of the wall may be described such that i) the layer with a low degree of compaction remained inside the backfill, ii) seepage water infiltrated into the soil layer, resulting in considerable amount of settlement due to "collapse" of the loosely compacted soil layer, and iii) the settlement caused large deformation on the wall facing.

Bearing this scenario in mind, some lessons learnt from this case study are described in the following:

i) the compaction curves of the local soils exhibited a variety in terms of the maximum dry density. Unfortunately, the compaction curve employed for the density control during filling showed the lowest value among them. Similar to the previous case study, care should be taken for the variation of the soil properties. Geotechnical engineers should not be immoral to deliberately choose a single compaction curve leading to low cost for the compaction work,

ii) the ground anchors with rigid concrete wall may be cost-effective countermeasure to prevent further development of wall deformation, and also to enhance the overall stability of the wall,

iii) the effects of the countermeasure on reducing not only the wall deformation but also the extensional strain of the geotextile may be confirmed by means of 2D and 3D numerical analysis, and

iv) moreover, the need to establish the performance-based design manual by properly considering stress-deformation behavior of geo-structure is urgently demanded for high-raised reinforced earth fill as such.

REFERENCES

Jung, M.S., Kawajiri, S., Hur, J.S., and Shibuya. S. (2010). Case study on severely-damaged reinforced soil retaining wall with geotextile in Hyogo, Japan, Part I: Site Investigation into the cause of damage, Proc. 3rd Korea-Japan Geotechnical Engineering Workshop, 3-10

Shibuya, S., Koseki, J. and Kawaguchi, T. (2005). Recent developments in deformation and strength testing of geomaterials, Keynote Lecture, Deformation Characteristics of Geomaterials-Recent Investigations and Prospects (Di Benedetto H. et al edns), Taylor Francis Group London, 3-28

Tatsuoka,F., Tateyama, M., Tamura, Y. and Yamauchi. H. (1997). Geosynthetic-reinforced soil retaining walls as important permanent structures, 1996-1997 Mercer Lecture, Geosynthetic International, 4(2), 21-136

Tatsuoka,F., Tateyama, M., Tamura, Y. and Yamauchi. H. (2000). Lessons from the failure of full-scale models and recent geosynthetic-reinforced soil retaining wall, Proc., the 2nd Asian Geosynthetics Conference, GeoAsia 2000, Kuala Lumpur, 1, 23-53